

**A GLOBAL HIGH RESOLUTION MAP OF THE MARTIAN HYDROGEN DISTRIBUTION** Luís F.A. Teodoro<sup>1</sup>, Richard C. Elphic<sup>2</sup>, Vincent R. Eke<sup>3</sup>, William C. Feldman<sup>4</sup>, Sylvestre Maurice<sup>5</sup>; <sup>1</sup> BAER, NASA Ames Research Center, Moffett Field, CA 94035-1000 (luis.f.teodoro@nasa.gov); <sup>2</sup> Planetary Systems Branch, Space Sciences and Astrobiology Division, MS 245-3, NASA Ames Research Center, Moffett Field, CA 94035-1000, USA; <sup>3</sup> Institute for Computational Cosmology, Department of Physics, Durham University, Science Laboratories, South Road, Durham DH1 3LE, UK; <sup>4</sup> Planetary Science Institute, 1700 E. Fort Lowell, Suite 106, Tucson, AZ, 85719, USA; <sup>5</sup> Université Paul Sabatier, Centre d'Etude Spatiale des Rayonnements, 9 avenue Colonel Roche, B.P. 44346 Toulouse, France

The Mars Science Laboratory (MSL) is a NASA mission that carries the most advanced suite of scientific instruments ever sent to the surface of Mars. Its main objective is to study whether Mars has been habitable at any point of its history. Such studies include the analysis of surficial soils and rocks to understand their mineralogical and chemical make up, additionally, the distribution of hydrogen in the top  $\sim 30$  cm of the surface at some locations of the Gale crater.

The European-Russian counterpart ExoMars (Exobiology on Mars) is also a planned Mars mission to search for possible biosignatures of Martian life, past and present. Additionally, it will also characterize the water geochemical environment as a function of depth in the shallow subsurface. This program will include orbitors as well as landers. The potential landing sites are *i*) Mawrth Vallis; *ii*) Nili Fossae; *iii*) Meridiani Planum; *iv*) Holden Crater; and *v*) Gale Crater.

Mars Odyssey carries a Neutron Spectrometer (MONS) that has been gathering information for more than a decade. When Galactic cosmic rays strike the surface of Mars, they generate neutrons from nuclei present in the top layer of the regolith by various nuclear reactions. Such neutrons lose energy by interacting with the surrounding nuclei and their flux leaking from the planet subsurface is thus an indication of the elemental composition of the top layer of the regolith as different elastic and inelastic scattering cross-sections produce different amounts of moderation and capture. For instance, hydrogen is especially effective at moderating neutrons [1]. This information therefore maps the global hydrogen distribution in the top few decimeters of the martian surface [2] (see Figure 1) and is complementary to the one that will be collected by MSL and ExoMars. In brief, deposits ranging between 20% and 100% Water-Equivalent Hydrogen (WEH) by mass are found pole-ward of 55 deg. latitude, and less rich, but still significant deposits are found at near-equatorial latitudes. Recently, [3] have re-analyzed the MONS epithermal data and significantly lowered the statistical systematic data re-

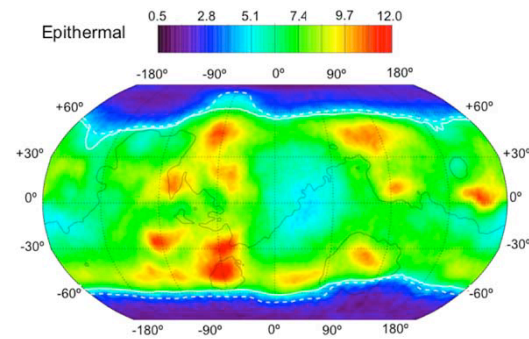


Figure 1: Epithermal  $\text{CO}_2$  frost-free map of Mars [3]. Data north of the white dashed wavy line were measured after the northern summer solstice ( $100^\circ < L_s < 151^\circ$ ) and data south of the southern dashed wavy line were measured during the late summer in the south ( $329^\circ < L_s < 1.7^\circ$ ). The 0-km elevation contour (black line) is shown for reference. The solid white lines separate the poleward regions having water abundances larger than about 11% by mass from those at near equatorial latitudes that have abundances that are less than 11%. The figure was extracted from Figure 1 in [2].

duction uncertainties that plagued previous versions of the data. However, MONS counting-rate data have a FWHM of  $\sim 550$  km, which is sufficiently broad to contain several Gale craters in it. In this study, we choose the PIXON numerical deconvolution technique [4, 5]. This algorithm removes the point spread function without introducing spurious features in the presence of noise. We have previously carried out a detailed study of the martian polar regions applying this methodology to Martian epithermal neutrons near both poles (e.g. [6]) and have been able to reach a resolution of  $\sim 45 - 100$  km. In the present study, we will apply this technique to the latest MONS epithermal  $\text{CO}_2$  frost-free data over the full surface of Mars.

To map the martian near-surface hydrogen distribution accurately is central to the study of volatiles delivery and retention in the terrestrial planets of the Solar System. It is also a crucial ingredient in the planning/management of current and future missions to the Mars surface.

**Pixon image reconstruction method:** In the presence of both some experimental noise,  $N$ , and instrumental blurring,  $B$ , the measured data,  $D$ , can be related to the input image,  $I$ , via

$$D = B * I + N, \quad (1)$$

where  $*$  denotes the convolution operator. The main goal of an image reconstruction algorithm is to choose a reconstruction,  $I'$ , that both avoids spurious complexity and produces a residual field,

$$R = D - B * I' \quad (2)$$

that is statistically equivalent to the anticipated experimental noise. The pixon reconstruction [7, 5] can be perceived as an “adaptive smoothing” technique with the scale of this smoothing set by the local information content in the data. Thus, each pixon, which can be thought of a set of spatially correlated pixels, contains the same information content. The reconstruction therefore looks smooth in this pixon basis and the image entropy is maximized.

In order to understand the statistical significance of the MONS results we use a Monte Carlo method, whereby mock data sets are created and then analyzed in exactly the same way as the data itself. To this end, 200 different mock realizations of the Mars Odyssey time series data are created, taking the MONS epithermal reconstructions as the input images,  $I$ . The different mocks vary only as a result of the random number chosen to add the noise. These mocks are also used to quantify possible systematic errors introduced by the reconstruction procedure.

**Preliminary Results:** In Figure 2 we present the epithermal neutron leakage reconstruction at the Gale Crater neighborhood in  $40 \times 40 \text{ km}^2$  pixels. For more details see figure caption. As for the north pole reconstruction (see Figure 3) the dynamical range and the sharpness of the features are enhanced. Although the reconstruction’s resolution is not as small as the polar counterparts (see Figure 3) it is still considerably smaller than the instrumental blurring ( $\sim 550 \text{ km}$ ).

**References:** [1] W. C. Feldman, et al. (1993) in *Remote Geochemical Analysis, Elemental and Mineralogical Composition*, ISBN 0521402816, Cambridge University Press, 1993. (Edited by C. M. Pieters, et al.). [2] W. C. Feldman, et al. (2004) *Journal of Geophysical Research (Planets)* 109(E18):9006 doi:10.1029/2003JE002160. [3] S. Maurice, et al. (2011) *Journal of Geophysical Research (Planets)* 116(E15):E11008

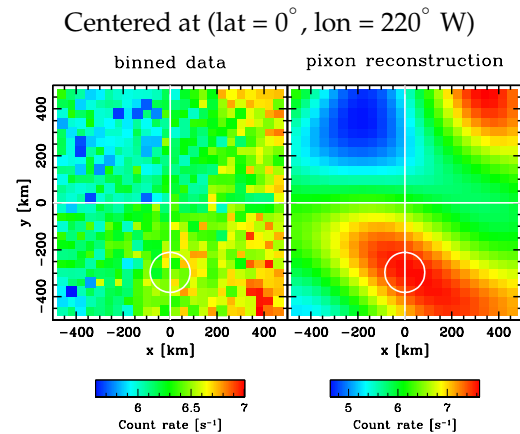


**Figure 2: Neutron count rate map at the Gale Crater neighborhood** From the left to the right we show the MONS data and pixon reconstructions in  $40 \times 40 \text{ km}^2$  bins. The white circle in the bottom half of the panels represent the Gale crater. The reconstruction is centered at (lat =  $0^\circ$ , lon =  $220^\circ$  W). The effective size of the MONS response function is  $\sim 550 \text{ km}$  (approximately the same size as the panels’ quadrants).

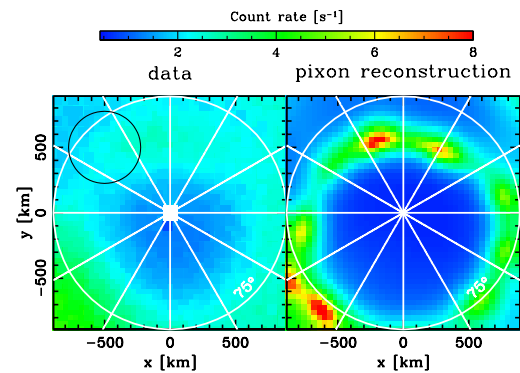


**Figure 3: Neutron count rate map at the North Pole** From the left to the right we show the MONS data and pixon reconstructions in  $40 \times 40 \text{ km}^2$  bins. The black circle shows the effective size of the MONS response function  $\sim 550 \text{ km}$ .

doi:10.1029/2011JE003810. [4] R. K. Pina, et al. (1993) *PASP* 105:630  
doi:10.1086/133207. [5] V. Eke (2001) *Mon. Not. R. Astron. Soc.* 324:108 doi:10.1046/j.1365-8711.2001.04253.x.  
[6] L. F. A. Teodoro, et al. (2010) *LPI Contributions* 1595:69. [7] R. K. Piña, et al. (1992) *PASP* 104:1096 doi:10.1086/133095.